

Re-entrant superconductivity in Nb/Cu_{1-x}Ni_x bilayers

V. Zdravkov¹, A. Sidorenko¹, G. Obermeier², S. Gsell², M. Schreck², C. Müller², S. Horn², R. Tidecks², L.R. Tagirov³

¹*Institute of Applied Physics, LISES ASM, Kishinev 2028, Moldova*

²*Institut für Physik, Universität Augsburg, D-86159 Augsburg, Germany*

³*Solid State Physics Department, Kazan State University, 420008 Kazan, Russia*

(Date textdate; Received textdate; Revised textdate; Accepted textdate; Published textdate)

We report on the first observation of a pronounced re-entrant superconductivity phenomenon in superconductor/ferromagnetic layered systems. The results were obtained using a superconductor/ferromagnetic-alloy bilayer of Nb/Cu_{1-x}Ni_x. The superconducting transition temperature T_c drops sharply with increasing thickness d_{CuNi} of the ferromagnetic layer, until complete suppression of superconductivity is observed at $d_{\text{CuNi}} \approx 4$ nm. Increasing the Cu_{1-x}Ni_x layer thickness further, superconductivity reappears at $d_{\text{CuNi}} \approx 13$ nm. Our experiments give evidence for the pairing function oscillations associated with a realization of the quasi-one dimensional Fulde-Ferrell-Larkin-Ovchinnikov (FFLO) like state in the ferromagnetic layer.

The coexistence of superconductivity (S) and ferromagnetism (F) in a homogeneous material, described by Fulde-Ferrell and Larkin-Ovchinnikov (FFLO) [1, 2], is restricted to an extremely narrow range of parameters [3]. So far no indisputable experimental evidence for the FFLO state exists.

In general, superconductivity and ferromagnetism do not coexist, since superconductivity requires the conduction electrons to form Cooper pairs with antiparallel spins, whereas ferromagnetism forces the electrons to align their spins parallel. This antagonism can be overcome if superconducting and ferromagnetic regions are spatially separated, as for example, in artificially layered superconductor/ferromagnet (S/F) nanostructures (see, e.g. [4], for an early review). The two long-range ordered states influence each other via the penetration of electrons through their common interface. Superconductivity in such a proximity system can survive, even if the exchange splitting energy $E_{\text{ex}} \sim k_B \theta_{\text{Curie}}$ in the ferromagnetic layer is orders of magnitude larger than the superconducting order parameter $\Delta \sim k_B T_c$, with T_c the superconducting transition temperature. Cooper pairs entering from the superconducting into the ferromagnetic region experience conditions drastically different from those in a non-magnetic metal. This is due to the fact that spin-up and spin-down partners in a Cooper pair occupy different exchange-split spin-subbands of the conduction band in the ferromagnet. Thus, the spin-up and spin-down wave-vectors of electrons in a pair, which have opposite directions, cannot longer be of equal magnitude and the Cooper pair acquires a finite pairing momentum [5]. This results in a pairing function that does not simply decay as in a non-magnetic metal, but in addition oscillates on a characteristic length scale. This length scale is the magnetic coherence length ξ_F , which will be specified below.

Various unusual phenomena follow from the oscillation of the pairing wave function in ferromagnets (see, e.g. the recent reviews [6, 7, 8] and references therein). A prominent example is the oscillatory S/F proximity effect. It

can be qualitatively described using the analogy with the interference of reflected light in a Fabry-Pérot interferometer at normal incidence. As the conditions change periodically between constructive and destructive interference upon changing the thickness of the interferometer, the flux of light through the interface of incidence is modulated. In a layered S/F system the pairing function flux is periodically modulated as a function of the ferromagnetic layer thickness d_F due to the interference. As a result, the coupling between the S and F layers is modulated, and T_c oscillates as a function of d_F .

The most spectacular evidence for the oscillatory proximity effect would be the detection of the re-entrant behavior of the superconducting transition temperature as a function of d_F , which has been predicted theoretically [9, 10, 11]. There is a sole report on the superconductivity re-entrance as a function of the ferromagnetic layer thickness in Fe/V/Fe trilayers [12]. Due to the very small thickness of the iron layers, at which the re-entrance phenomenon is expected (0.7-1.0 nm, i.e. 2-4 monolayers of iron only), the number of the experimental points $T_c(d_F)$ is very small, with a large scattering of the results.

The oscillation length $\xi_F = \hbar v_F / E_{\text{ex}}$ in strong ferromagnets, like iron, nickel or cobalt, is extremely short, because the exchange splitting energy E_{ex} of the conduction band is in the range 0.1-1.0 eV [4]. Here, v_F is the Fermi velocity in the F material and \hbar Planck's constant. Ferromagnetic alloys, with E_{ex} an order of magnitude smaller, allow the observation of the effect at larger thicknesses d_F of about 5-10 nm. Such layers can be easier controlled and characterized. Another advantage using ferromagnetic alloys is that for a long-wavelength oscillation the atomic-scale interface roughness has no longer a decisive influence on the extinction of the T_c oscillations.

The S/F proximity effect has not only been studied using elemental ferromagnetic materials, but also for various ferromagnetic alloys [13, 14, 15, 16, 17, 18, 19]. A non-monotonic dependence of T_c vs. d_F has been observed. In the present work, Nb was chosen as a su-

perconductor and a $\text{Cu}_{1-x}\text{Ni}_x$ alloy with $x \approx 0.59$ for the ferromagnetic layer. In this alloy the magnetic momentum and Curie temperature show an almost linear dependence on the Ni concentration [20]. For $x \approx 0.59$ we find $\theta_{\text{Curie}} \approx 170$ K.

The samples were prepared by magnetron sputtering on commercial (111) silicon substrates at 300 K. The base pressure in the “Leybold Z400” vacuum system was about 2×10^{-6} mbar, pure argon (99.999%, “Messer Griesheim”) at a pressures of 8×10^{-3} mbar was used as sputter gas. Three targets, Si, Nb and $\text{Cu}_{1-x}\text{Ni}_x$ (75 mm in diameter), were pre-sputtered for 10-15 minutes to remove contaminations from the targets as well as to reduce the residual gas pressure from the chamber during the pre-sputtering of Nb, which acts as a getter material. Then, we first deposited a silicon buffer layer, using a RF magnetron to generate a clean interface for the subsequently deposited niobium layer. To average over spatial differences of the sputtering characteristics, we moved the target during the DC sputtering process of the Nb layer, obtaining a smooth Nb film of constant thickness d_{Nb} . The average growth rate of the Nb film was about 1.3 nm/sec, while the rate of the sputtering process was adjusted to 4 nm/sec, to reduce the amount of contaminations gettered into the Nb film. The $\text{Cu}_{1-x}\text{Ni}_x$ target [21] was RF sputtered (rate 3 nm/sec) resulting in the same composition of the alloy in the film. As in our previous work [22] we deposited a wedge-shaped ferromagnetic layer to obtain a series of samples with varying ferromagnetic $\text{Cu}_{1-x}\text{Ni}_x$ layer thickness. To prepare this wedge, the 80 mm long and 7 mm wide silicon substrate was mounted at a distance of 4.5 cm from the $\text{Cu}_{1-x}\text{Ni}_x$ target symmetry axis to utilize the intrinsic spatial gradient of the deposition rate. To prevent the degradation of the Nb/ $\text{Cu}_{1-x}\text{Ni}_x$ bilayers at atmospheric conditions, the bilayers were coated by a silicon layer of about 5 nm thickness. A sketch of the resulting wedge-like samples is presented in the inset of Fig. 1. Samples of equal length and width were cut from the wedge to obtain a set of 2.5 mm wide strips with varying $\text{Cu}_{1-x}\text{Ni}_x$ layer thickness. Aluminum wires of 50 μm in diameter were then attached to the strips by ultrasonic bonding for four-probe resistance measurements. Two batches of samples were prepared, one with $d_{\text{Nb}} \approx 7.3$ nm (S15), the other with $d_{\text{Nb}} \approx 8.3$ nm (S16).

After characterizing the samples by resistance measurements, Rutherford backscattering spectrometry (RBS) has been used to evaluate the thickness of the Nb and $\text{Cu}_{1-x}\text{Ni}_x$ layers as well as to check the concentration of Cu and Ni in the deposited alloy layers (Fig. 1). The applicability of this method for thickness determination has been demonstrated in our previous work [22]. It allows determining the thickness (via the areal density) of the layers with an accuracy of $\pm 3\%$ for $\text{Cu}_{1-x}\text{Ni}_x$ on the thick side of the $\text{Cu}_{1-x}\text{Ni}_x$ wedge, and $\pm 5\%$ for Nb and $\text{Cu}_{1-x}\text{Ni}_x$ on the thin side of the wedge. The

measurements were performed with 3.5 MeV He^{++} ions delivered by a tandem accelerator. The backscattered ions were detected under an angle of 170° with respect to the incident beam by a semiconductor detector. In order to avoid channeling effects in the Si substrate, the samples were tilted by 7° and azimuthally rotated during the measurement. The spectra were simulated using the RUMP computer program [23]. From the deduced elemental areal densities of Nb and $\text{Cu}_{1-x}\text{Ni}_x$ alloy the thickness of the two layers was calculated using the densities of the respective metals. The results for the layer thickness and $\text{Cu}_{1-x}\text{Ni}_x$ alloy composition as a function of position on the substrate of batch S15 are shown in Fig. 1. The Ni concentration in the $\text{Cu}_{1-x}\text{Ni}_x$ layer is nearly constant showing a slight increase towards the thick side of the wedge. The thickness of the Nb layer is nearly constant along the wedge, $d_{\text{Nb}}(\text{S15}) \approx 7.3$ nm.

The resistance measurements were performed in a ^3He cryostat and a dilution refrigerator. The standard DC four-probe method was used, applying a sensing current of 10 μA in the temperature range 0.4 K-10 K and of 2 μA in the range 10 mK-1.0 K, respectively. The polarity of the current was alternated during the resistance measurements to eliminate possible thermoelectric voltages. The superconducting critical temperature T_c was determined from the midpoints of the $R(T)$ curves at the superconducting transition (Fig. 2). The transition width (defined by the temperature interval in which the resistance changes from $0.1R_n$ to $0.9R_n$, with R_n the normal state resistance just above the transition) was below 0.2 K for most of the investigated samples. The shift between transition measured for increasing and decreasing temperature was smaller than 15 mK.

Figure 3 demonstrates for two values of the Nb layer thickness ($d_{\text{Nb}} \approx 8.3$ nm in Fig. 3a and $d_{\text{Nb}} \approx 7.3$ nm in Fig. 3b) the dependence of the superconducting transition temperature on the thickness of the $\text{Cu}_{1-x}\text{Ni}_x$ layer. For specimens with $d_{\text{Nb}} \approx 8.3$ nm the transition temperature T_c reveals a non-monotonic behavior with a deep minimum at about $d_{\text{CuNi}} \approx 7.0$ nm. For $d_{\text{Nb}} \approx 7.3$ the transition temperature decreases sharply upon increasing the ferromagnetic $\text{Cu}_{1-x}\text{Ni}_x$ layer thickness, till $d_{\text{CuNi}} \approx 3.8$ nm. Then, in the range $d_{\text{CuNi}} \approx 4.0 - 12.5$ nm, the superconducting transition temperature vanishes (at least T_c is lower than the lowest temperature measured in our cryogenic setup, *i.e.* 40 mK). For $d_{\text{CuNi}} > 12.5$ nm a superconducting transition is observed again with T_c increasing up to about 2 K. This phenomenon of re-entrant superconductivity is the most important finding of the present study.

For the regions of values of d_{CuNi} for which T_c changes rapidly, the transition width is broader than 0.2 K, and the $R(T)$ curve appears slightly asymmetric with respect to the midpoint of the transition. This is probably due to the small variation of the thickness of the ferromagnetic layer within each sample, since they were cut from

a wedge as described above.

To compare the prediction of the theory for the $T_c(d_F)$ dependence of Tagirov [10] with our experimental results, we followed closely the fitting procedure described in detail in reference [22]. The calculated curves of $T_c(d_F)$ in Fig. 3 (a) and (b) agree qualitatively well with the measured values. The electron mean free path $l_F \approx 15$ nm for the ferromagnetic material used for the calculations appears surprisingly long for an alloy, in particular, since a value of $l_F \approx 4.4$ nm, was inferred from resistivity measurements on a $\text{Cu}_{1-x}\text{Ni}_x$ alloy with $x \approx 0.51$ [17]. The reason could be a more complicated character of the diffusion of Cooper pairs in the F material and its temperature dependence in such type of S/F-system than considered by the present version of the theory. The small cusp-like structure in the $T_c(d_{\text{CuNi}})$ dependence at $d_{\text{CuNi}} \approx 1$ nm cannot be explained by the existing theoretical approaches, *i.e.* neither the single-mode nor the multi-mode approximation [24, 25] can account for this structure. We presume that the case $d_{\text{CuNi}} < \xi_F, l_F$ needs special consideration in the framework of the “pure limit” theoretical approach [11].

In conclusion, we present the first conclusive experimental observation of re-entrant behavior of superconductivity and large-amplitude oscillations of the superconducting T_c , in two series of superconductor/ferromagnet bilayers with constant Nb layer thickness ($d_{\text{Nb}} \approx 7.3$ nm and $d_{\text{Nb}} \approx 8.3$ nm) as a function of the thickness of a $\text{Cu}_{1-x}\text{Ni}_x$ ($x \approx 0.59$) alloy layer.

The authors are grateful to V. Ryazanov and V. Oboznov for stimulating discussions and cooperation, and to Yu. Shalaev for technical assistance in constructing the target-holder movement setup. The work was partially supported by INTAS (grant YSF 03-55-1856) and BMBF (project MDA02/002).

-
- [1] P. Fulde and R. Ferrell, Phys. Rev. **135**, A550 (1964).
 - [2] A. I. Larkin and Yu. N. Ovchinnikov, Zh. Eksp. Teor. Fiz. **47**, 1136 (1964) [Sov. Phys. JETP **20**, 762 (1965)].
 - [3] P. Fulde, Adv. Phys. **22**, 667 (1973), Fig. 22.
 - [4] C. L. Chien and D. H. Reich, J. Magn. Magn. Mater. **200**, **83** (1999).
 - [5] E. A. Demler, G. B. Arnold, and M. R. Beasley, Phys. Rev. B **55**, 15174 (1997).
 - [6] A. A. Golubov, M. Yu. Kupriyanov, and E. Il'ichev, Rev. Mod. Phys. **76**, 411 (2004).
 - [7] I. F. Lyuksyutov and V. L. Pokrovsky, Adv. Phys. **54**, 67 (2005).

- [8] A. I. Buzdin, Rev. Mod. Phys. **77**, 935 (2005).
- [9] M. G. Khusainov and Yu. N. Proshin, Phys. Rev. B **56**, R14283 (1997); Erratum: Phys. Rev. B **62**, 6832 (2000).
- [10] L. R. Tagirov, Physica C **307**, 145 (1998).
- [11] B. P. Vodopyanov and L. R. Tagirov, ZhETF Pis'ma **78**, 1043 (2003) [JETP Letters **78**, 555 (2003)].
- [12] I. A. Garifullin, D. A. Tikhonov, N. N. Garif'yanov, L. Lazar, Yu. V. Goryunov, S. Ya. Khlebnikov, L. R. Tagirov, K. Westerholt, and H. Zabel, Phys. Rev. B **66**, 020505(R) (2002).
- [13] L. V. Mercaldo, C. Attanasio, C. Coccorese, L. Maritato, S. L. Prischepa, and M. Salvato, Phys. Rev. B **53**, 14040 (1996).
- [14] M. Schöck, C. Sürgers, and H. v. Löhneysen, Eur. Phys. J. B **14**, 1 (2000).
- [15] J. Y. Gu, C.-Y. You, J. S. Jiang, J. Pearson, Ya. B. Bazaliy, and S. D. Bader, Phys. Rev. Lett. **89**, 267001 (2002).
- [16] V. V. Ryazanov, V. A. Oboznov, A. S. Prokofiev, and S. V. Dubonos, JETP Letters **77**, 39 (2003) [Pis'ma v ZhETF **77**, 43 (2003)].
- [17] A. Potenza and C. H. Marrows, Phys. Rev. B **71**, 180503 (2005).
- [18] Jinho Kim, Jun Hyung Kwon, K. Char, Hyeonjin Doh, and Han-Yong Choi, Phys. Rev. B **72**, 014518 (2005).
- [19] C. Cirillo, S. L. Prischepa, M. Salvato, C. Attanasio, M. Hesselberth, and J. Aarts, Phys. Rev. B **72**, 144511 (2005).
- [20] S. V. Vonsovskii, *Magnetism* (John Wiley, New York, 1974).
- [21] The $\text{Cu}_{1-x}\text{Ni}_x$ target with $x = 0.58 - 0.59$ was fabricated in the laboratory of Prof. V. V. Ryazanov, ISSP of RAS, Chernogolovka.
- [22] A. S. Sidorenko, V. I. Zdravkov, A. Prepelitsa, C. Helbig, Y. Luo, S. Gsell, M. Schreck, S. Klimm, S. Horn, L. R. Tagirov, and R. Tidecks, Annalen der Physik (Leipzig-Berlin) **12**, 37 (2003).
- [23] L. R. Doolittle, Nucl. Instr. Meth. B **9**, 344 (1985).
- [24] Ya. V. Fominov, N. M. Chitchev, and A. A. Golubov, Phys. Rev. B **66**, 014507 (2002).
- [25] Chun-Yeol You, Ya. B. Bazaliy, J. Y. Gu, S.-J. Oh, L. M. Litvak, and S. D. Bader, Phys. Rev. B **70**, 014505 (2004).

Figure captions

Fig. 1. The results of a Rutherford backscattering spectrometry (RBS) investigation: S15 batch, $d_{\text{Nb}} \approx 7.3$ nm.

Fig. 2. Typical resistive transitions of the investigated samples. Solid lines are a guide to the eye.

Fig. 3. Nonmonotonous $T_c(d_F)$ dependence for Nb/ $\text{Cu}_x\text{Ni}_{1-x}$ bilayers: (a) $d_{\text{Nb}} \approx 8.3$ nm; (b) $d_{\text{Nb}} \approx 7.3$ nm. Transition widths are within the point size if error bars are not visible. Solid lines are theoretical curves (see text).

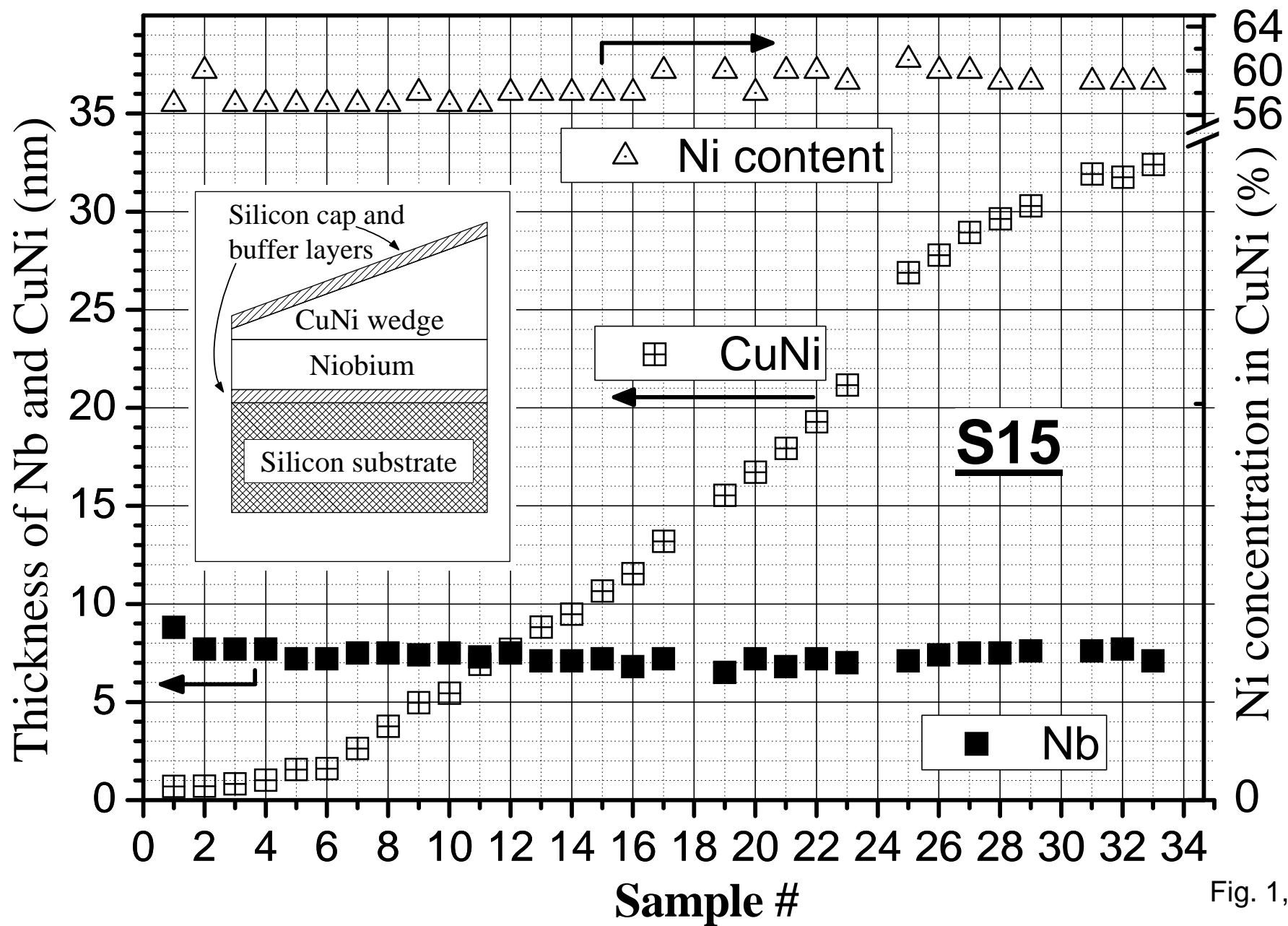


Fig. 1,
 V. Zdravkov *et al.*

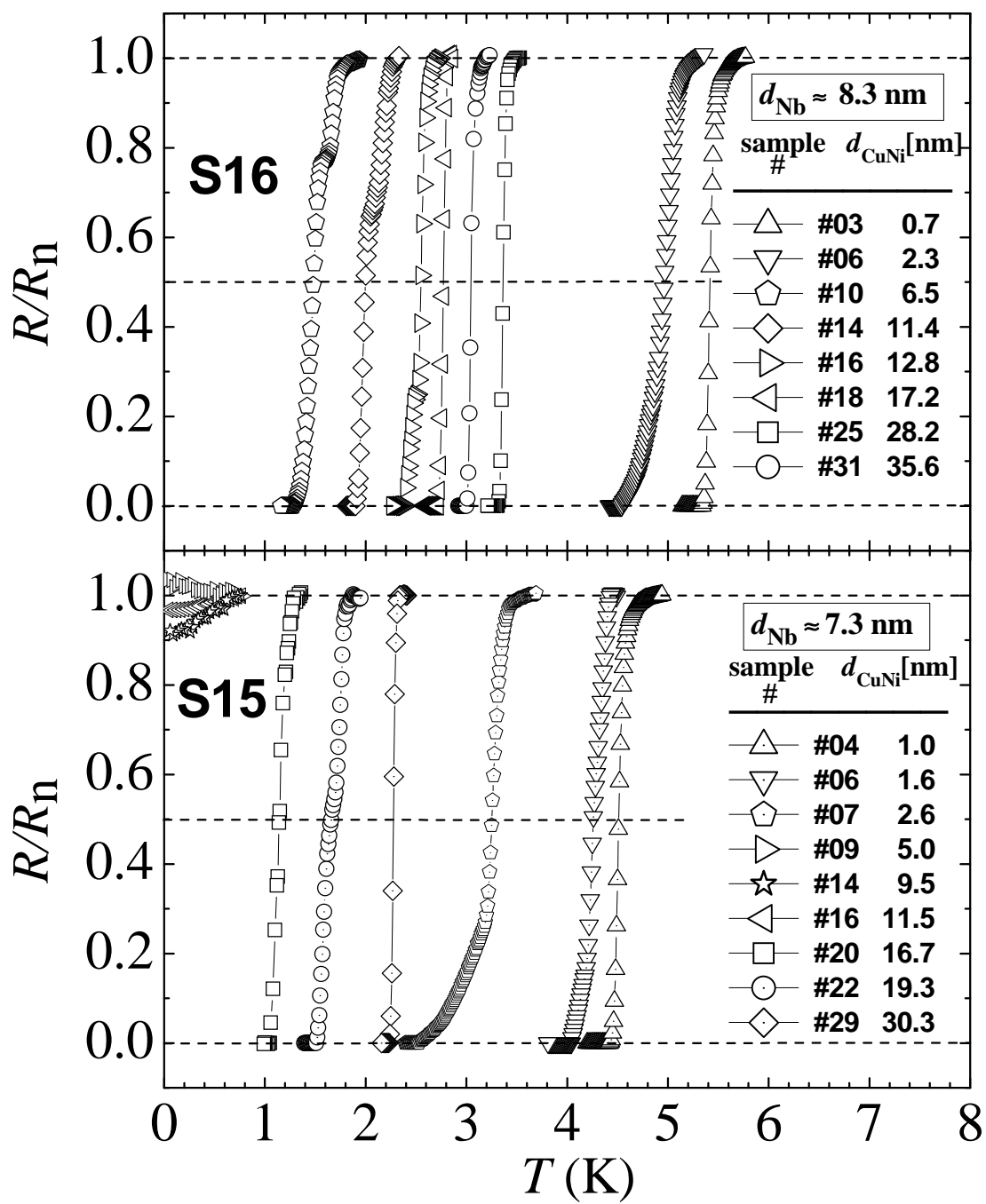


Fig. 2,
V. Zdravkov *et al.*

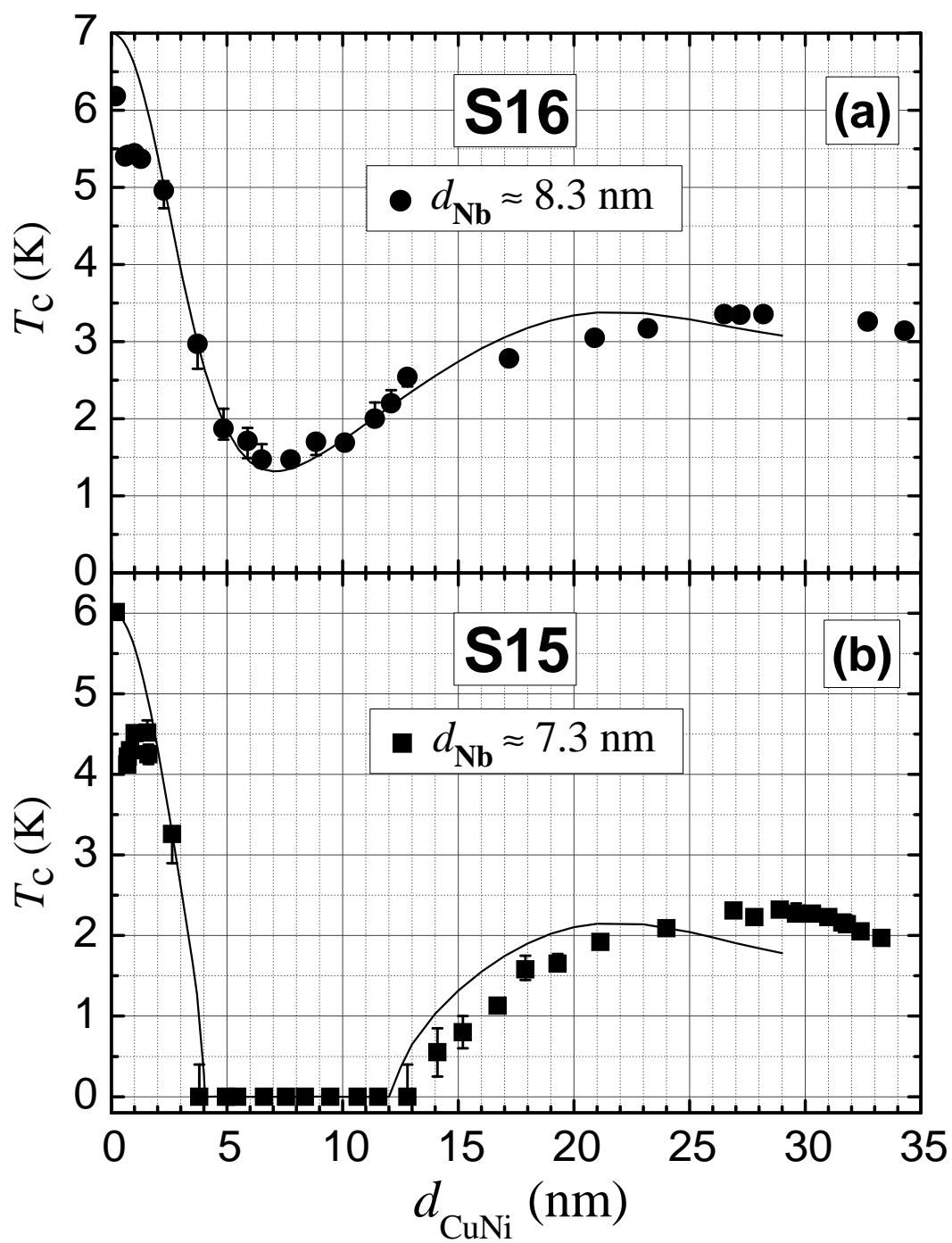


Fig. 3,
V. Zdravkov *et al.*